SECURITY INFORMATION
UNCLASSIFIED CONFIDENTIAL

Copy 6
RM E52G03

NACA RM E52G03

RESEARCH MEMORANDUM

EFFECT OF ROTOR- AND STATOR-BLADE MODIFICATIONS ON SURGE PERFORMANCE OF AN 11-STAGE AXIAL-FLOW COMPRESSOR

I - ORIGINAL PRODUCTION COMPRESSOR OF XJ40-WE-6 ENGINE

By Harold B. Finger, Robert H. Essig, and E. William Conrad

Lewis Flight Propulsion Laboratory
Cleveland, Ohio

CLASSIFICATION CHANGED
To UNCLASSIFIED
By authority of Naca PA 2 Date 10-31-58
MB 1-7-59

CLASSIFIED DOCUMENT

This material contains information affecting the National Defense of the United States within the meaning of the espionage laws, Title 18, U.S.C., Secs. 793 and 794, the transmission or revelation of which in any manner to an unauthorized person is prohibited by law.

NATIONAL ADVISORY COMMITTEE FOR AERONAUTICS
WASHINGTON
May 20, 1953

CONFIDENTIAL
UNCLASSIFIED
NACA LIBRARY

UNCLASSIFIED

NASA Technical Library
3 1176 01435 6118

[redacted]

NATIONAL ADVISORY COMMITTEE FOR AERONAUTICS

RESEARCH MEMORANDUM

EFFECT OF ROTOR- AND STATOR-BLADE MODIFICATIONS ON SURGE PERFORMANCE OF AN 11-STAGE AXIAL-FLOW COMPRESSOR

I - ORIGINAL PRODUCTION COMPRESSOR OF XJ40-WE-6 ENGINE

By Harold B. Finger, Robert H. Essig, and E. William Conrad

2616

SUMMARY

An investigation to increase the compressor surge-limit pressure ratio of the XJ40-WE-6 turbojet engine at high equivalent speeds was conducted at the NACA Lewis altitude wind tunnel. This report evaluates the compressor modifications which were restricted to (1) twisting rotor blades (in place) to change blade section angles and (2) inserting new stator diaphragms with different blade angles. Such configuration changes could be incorporated quickly and easily in existing engines at overhaul depots.

It was found that slight improvements in the compressor surge limit were possible by compressor blade adjustment. However, some of the modifications also reduced the engine air flow and hence penalized the thrust. A mixer assembly designed and supplied by the engine manufacturer was used at the compressor outlet and improved the surge limit with no appreciable thrust penalty.

INTRODUCTION

Preliminary performance tests of the XJ40-WE-6 turbojet engine in the NACA Lewis altitude wind tunnel revealed a severe compressor surge limitation at high equivalent engine speeds. This surge limit imposed a thrust reduction on the engine of approximately 20 percent below the expected value. Almost simultaneously the same difficulty was reported by an airframe manufacturer using this engine in a prototype airplane. The problem had not been encountered previously, because the engine manufacturer did not have facilities for supplying the cold air required for high equivalent engine speeds.

[redacted]

UNCLASSIFIED

A program to increase the surge-limit pressure ratio of the XJ40-WE-6 engine was immediately initiated. In view of the fact that production had been started and a small number of engines were already in the field, the objectives of the surge program were twofold: (a) to remove the thrust limitation resulting from compressor surge on existing engines by compressor modifications which could be quickly and conveniently incorporated on engines in the field and (b) to provide, for future production engines, a compressor configuration with good efficiency and air-flow characteristics which would operate without surge at all flight conditions. In objective (a) slight sacrifices in efficiency and air flow were permissible if the high-altitude operation required by the prototype-airplane programs dependent upon this engine could be obtained.

2616

The methods considered for improving the surge limit without major rework of the compressor were as follows:

(1) Twisting rotor blades (in place) to change blade section angles

(2) Inserting new stator diaphragms with different blade angles

(3) Increasing the turbine-nozzle flow area to permit the compressor to operate at lower pressure ratios

The effect of increasing turbine-nozzle area will be considered in a later report. The results of blade-angle changes (1) and (2) are presented in the present report. Each compressor configuration is evaluated primarily by its surge limit over a range of equivalent engine speeds, but consideration is also given to air flows and efficiencies.

APPARATUS AND PROCEDURE

Description of Engine

The engine discussed herein was designated as an XJ40-WE-6 engine as received; however, it must be regarded as a prototype because of modifications included later as a result of this study. The design static sea-level performance was 7500 pounds thrust at an engine speed of 7260 rpm and a turbine-inlet gas temperature of 1425° F. Compressor pressure ratio was 5 to 1 at an air weight flow of 140 pounds per second. Main components of the engine (fig. 1) were an 11-stage axial-flow compressor, a single-annular combustor, a two-stage turbine, an exhaust collector, and a continuously variable clam-shell-type exhaust nozzle. Over-all length of the engine was 186 inches; height and width of the engine, including accessories, were 45.5 inches and 42.4 inches, respectively; and the dry weight was 2981 pounds. Primary control of the engine was accomplished electronically, with an hydraulic control providing emergency protection.

[redacted]

Air ducting to the compressor consisted of two elliptical engine inlets, one on either side of the accessory gear case as shown in figure 2. The air passages joined to form an annulus approximately 2 inches ahead of the inlet guide vanes. A view of the compressor with the top half of the casing removed is shown in figure 3. The 11-stage rotor was followed by two rows of outlet guide vanes to provide axial flow into the combustor. During part of this investigation a "mixer" section, supplied by the engine manufacturer, was substituted for the second row of outlet guide vanes. The mixer consisted essentially of twisted guide vanes where adjacent blades were twisted in opposite directions. The purpose of the mixer was to intermix the high-energy air at the rotor tip with the low-energy air at the root in an effort to control radial temperature distribution at the turbine inlet.

2616

A variable-area first-stage turbine-nozzle diaphragm (fig. 4) was also supplied by the manufacturer. The diaphragm proved to be an excellent research tool in that it permitted steady-state operation at compressor pressure ratios up to the surge limit without exceeding turbine temperature limitations. Thus, surge limits of the various compressor configurations could be obtained rapidly and accurately. It also provided a means of evaluating directly the effect of increasing turbine-nozzle area and hence rematching the compressor and the turbine.

Installation

As shown in figure 1, the engine was mounted on a wing spanning the test section of the altitude wind tunnel. Dry refrigerated air was supplied to the engine from the tunnel make-up air systems through a duct connected to the engine inlet. Manually controlled butterfly valves in this duct were used to adjust total air pressures at the engine inlet. A slip joint with a frictionless seal was used in the duct, which made possible the measurement of thrust and drag with the tunnel scales.

Instrumentation for measuring pressures and temperatures was installed at various stations in the engine (fig. 5) to determine the steady-state performance. A schematic diagram showing location of typical instrumentation in the compressor is given in figure 6. A traverse mechanism comprising 10 sonic-type thermocouples (reference 1) was supplied by the engine manufacturer to determine the gas-temperature pattern at the turbine inlet. Transient instrumentation similar to the type described in reference 2 was installed in order to observe the nature of the surge.

Procedure

Symbols and methods of calculation are given in appendixes A and B, respectively. The air flow through the make-up air duct was throttled from approximately sea-level pressure to a total pressure at the engine inlet corresponding to the desired flight Mach number at a given altitude. The static pressure in the tunnel test section was maintained to correspond to the desired altitude. Engine inlet-air temperatures were held at approximately NACA standard values corresponding to the simulated flight conditions, except for high altitudes and low flight Mach numbers. No inlet-air temperatures below about -20° F were obtained.

2616

The first engine configuration had surge characteristics such that it was necessary to operate at turbine-outlet temperatures below military at high equivalent engine speeds to avoid compressor surge. Consequently, it was possible to determine the compressor surge limits simply by closing the exhaust nozzle at constant engine speed until surge occurred. For later configurations where the surge limit was above the limiting temperature operating line with the standard turbine area, the variable-area turbine nozzle was used to allow operation up to the surge limit without encountering limiting turbine temperature. The effect of changes in turbine area on the relation between compressor pressure ratio and turbine-inlet temperature is given in figure 7.

Most of the surge data were obtained at equivalent engine speeds between 4800 and 8000 rpm at an altitude of 30,000 feet and a flight Mach number of 0.64. In addition, surge data were obtained on several configurations at altitudes of 15,000 and 45,000 feet and flight Mach numbers of 0.53 and 0.21, respectively, to determine the effects of varying flight conditions.

Compressor Design Analysis

The compressor of the XJ40-WE-6 turbojet engine is an 11-stage unit having an inlet hub-tip ratio of 0.6. It was initially designed to handle an air weight flow of 136.2 pounds per second at a pressure ratio of 4.6 and a speed of 7260 rpm. Mismatching between the compressor and the turbine was encountered at the start of the development program, and the compressor stator and rotor blades were reset by the manufacturer so as to shift the design point to a pressure ratio of 5 and the air flow to 140 pounds per second. The typical stage of the compressor was designed for a symmetrical velocity diagram at all radii.

The axial velocity distributions assumed throughout the compressor were based on experimental data previously obtained by the manufacturer. This flow distribution is set up in the first two stages, which impart a work gradient from root to tip. This increase in enthalpy from hub to tip is gradually equalized through the compressor by reversing the work distribution in the stages beyond the second stage.

The design axial-velocity distributions at the inlet to each rotor row in the compressor are presented in figure 8. The design axial velocity decreases rapidly in the first two stages, which have a constant annular area, and then decreases gradually through the remainder of the compressor.

2616

The design of the first three and last three stages neglects simple radial-equilibrium requirements. Inlet guide-vane investigations (reference 3) and unpublished single-stage compressor data have indicated that simple radial-equilibrium conditions are satisfied, at least at the inlet to the first rotor. Therefore the actual incidence-angle distributions differ appreciably from the design values. Conditions downstream of the first rotor have been found to approximate a condition between straight through-flow and simple radial equilibrium (reference 4), and recent single-stage results have indicated a condition closer to simple equilibrium than to straight through-flow behind the rotor.

In order to determine the general effect of neglecting simple radial equilibrium on the operation of the first rotor, calculations of axial velocity and rotor angle of attack were made in which it was assumed that the flow left the inlet guide vanes at the guide-vane trailing-edge angle and that simple radial equilibrium was satisfied. These velocity calculations were based on the original design weight flow of 136.2 pounds per second. Comparison of the results of these calculations with the design data is presented in figure 9. The computed axial velocity is lower than the design velocity over the major portion of the flow passage with the exception of the region near the hub where the calculated axial velocity is higher than design. As a result of the distribution of axial velocity, the calculated rotor angle of attack is approximately 10° higher than the design value at the tip and approximately 4° lower at the hub. These data lead to the conclusion that the tip section may be stalled at design speed, and the hub section may be approaching a turbining condition.

Redesign of the inlet stages of the compressor more nearly to approximate radial equilibrium is therefore essential, if improved performance is to be obtained. Reduction in the angle of attack at the first rotor tip should improve low-speed performance characteristics

of the compressor because of the high angles encountered at speeds below design. The interstage data which were obtained during the investigation indicated the critical operation of the hub section of the inlet stages over the entire range of conditions investigated.

Because the exit-stage blade heights were small and because conditions at the inlet to these stages were not accurately determinable by the design method, it was felt that the errors involved as a result of neglecting radial equilibrium in these stages were small. This belief has been substantiated by preliminary velocity calculations in the exit stages.

2616

Compressor Modifications

When the initial compressor design point was shifted to a higher pressure ratio and weight flow, the margin that existed between the high-speed stable operating line and the surge limit was apparently eliminated. Several quick methods for increasing the surge limit of the compressor without major modification were considered. The analysis of reference 5 indicates that slight changes may be made in the low-speed performance of a high-pressure-ratio compressor by resetting blade angles. Extension of the analysis to the present high-speed surge problem indicated that compressor surge above design speed generally results from stall caused by high angle of attack at the exit stages. In an attempt to unload the exit stages, Westinghouse and NACA personnel mutually agreed to limit compressor modifications to

(1) Twisting rotor blades (in place) to change blade section angles

(2) Inserting new stator diaphragms with different blade angles

On the basis of the analysis of reference 5 and the experimental results obtained with the standard compressor, a series of successive blade modifications was made. The resulting configurations are listed in the following table, which indicates changes in blade-angle settings from the standard compressor. A description of the various compressor configurations, all with the discharge mixer installed, and the objective of each modification follow:

Configuration A. - For configuration A, designated as standard, the compressor as received from the manufacturer was installed in the engine with the mixer assembly and the variable-area turbine-nozzle diaphragm.

Configuration B. - In configuration B, standard blade angles were used throughout with the exception of the ninth and eleventh rotor rows. These blade rows were twisted closed from the tip by the amounts

Configuration	Radial position	Blade-angle modifications (deg)[1]											
		Inlet guide vane	First rotor	First stator	Second rotor	Second stator	Third stator	Seventh stator	Eighth stator	Ninth rotor	Ninth stator	Tenth stator	Eleventh rotor
A	Hub Mean Tip	STANDARD[2]											
B	Hub	Std	Std	Std	Std	Std	Std	Std	Std	Std	Std	Std	Std
	Mean	Std	Std	Std	Std	Std	Std	Std	Std	-1.5	Std	Std	-3
	Tip	Std	Std	Std	Std	Std	Std	Std	Std	-3	Std	Std	-6
C	Hub	Std	Std	Std	Std	Std	Std	-3	-3	Std	-3	-3	Std
	Mean	Std	Std	Std	Std	Std	Std	-3	-3	-1.5	-3	-3	-3
	Tip	Std	Std	Std	Std	Std	Std	-3	-3	-3	-3	-3	-6
D	Hub	Std	Std	1.8	Std	0.3	-1.6	-3	-3	Std	-3	-3	Std
	Mean	Std	-3.5	-2.5	-1.5	- .2	1.6	-3	-3	-1.5	-3	-3	-3
	Tip	Std	-7	-3.4	-3	-2.0	-2.3	-3	-3	-3	-3	-3	-6
E	Hub	Std	Std	1.8	Std	0.3	-1.6	-3	-3	Std	-3	-3	Std
	Mean	Std	-3.5	-2.5	-1.5	- .2	1.6	-3	-3	Std	-3	-3	Std
	Tip	Std	-7	-3.4	-3	-2.0	-2.3	-3	-3	Std	-3	-3	Std

[1]Negative angles indicate decreasing angle between the blade chord and the tangential direction.
[2]Original blade settings with discharge mixer installed, designated standard in this table.

indicated in the table. The objective of this modification was to unload these exit stages at the tip by the direct effect of the twisting and at the hub by the indirect effect of shifting the flow inward. It was also felt that the radial equilibrium relation, which effect is believed to be small for these short blades, would be somewhat better satisfied in the exit stages by such a modification.

Configuration C. - Configuration C was the same as configuration B, except that the stators in the seventh to the tenth stages were closed 3°, a modification which unloaded these stators and the following rotors. A preliminary analysis has indicated that resetting a row of stator blades a constant amount from hub to tip alters the angle of attack on the following rotor a greater amount at the hub than at the tip section. It was expected that such a modification would increase the problems associated with acceleration and operation at speeds below design.

2616

Configuration D. - Configuration D was the same as configuration C with the exception of the inlet stages. The tip sections of the first three rotors were unloaded and the hub sections of the second and third rotors were loaded in order to approximate more closely the angles required for the radial-equilibrium condition, which was found to have an appreciable effect on the velocity diagrams in these inlet stages. It was expected that this modification would appreciably improve performance in the range of speeds near design speed as a result of setting the blade sections in the inlet stages closer to the peak efficiency points. It should be emphasized that this modification did not alter the angle of attack or blade-angle setting at the hub of the first rotor, which was found to be turbining in the design analysis.

Configuration E. - For configuration E, the rotor blades in the ninth and eleventh stages were retwisted to the settings in the standard compressor (configuration A). This change was based upon the results of the investigation of configuration B.

In addition to the changes made in the blade-angle settings, configurations A and E were run with various combinations of the compressor-discharge mixer, standard outlet guide vanes, and the standard fixed-area turbine-nozzle diaphragm. The modifications which were used to investigate the effects of these auxiliary blade rows are listed in the following table:

Configuration	Outlet guide vane	Turbine nozzle
A	Mixer	Variable-area
A1	Standard	Standard
E	Mixer	Variable-area
E1	Standard	Standard
E2	Mixer	Standard

[redacted]

Configuration A1 had the same compressor blade angles as those of configuration A. Configurations E1 and E2 had the same blade-angle specifications as configuration E. Thus comparison of the performance of the E configurations presents the effects of the discharge mixer and the variable-area turbine nozzle, while comparison of configurations A1 and E1 presents the improvements made in the compressor as a result of the blade-angle adjustments.

RESULTS AND DISCUSSION

Effect of Surge Limit on Engine Performance

The severe thrust limitation imposed upon the engine by compressor surge at high equivalent speeds is illustrated graphically by figure 10. The military operating line intersects the surge limit, which is shown as a shaded area because it could not be obtained more precisely. The surge limit is unusual in that it occurs at an essentially constant pressure ratio over a wide range of equivalent engine speeds. Altitude has little effect on the surge limit; and below about 35,000 feet, Reynolds number effects on the engine operating line are small. Hence figure 10 represents the relation between the operating line and the surge limit for all altitudes to approximately 35,000 feet. Thus the increase in equivalent engine speed as the altitude is increased from sea level causes the operating point at military power to approach and finally encounter surge. For the original engine, therefore, it was possible to maintain military power only at equivalent engine speeds below approximately 7600 rpm or at stagnation air temperatures above 10° F. Further increases in corrected speed caused by reductions in ambient-air temperature required that the exhaust nozzle be opened to avoid surge. Opening the exhaust nozzle reduced the turbine-inlet temperature and hence the thrust available. The surge limit might also be avoided by reducing actual engine speed at constant exhaust-nozzle area; however, thrust losses would still be high.

Performance Map of Original Compressor with Mixer

In an effort to avoid adverse temperature profiles at the turbine inlet during the program to improve the surge limit, both the mixer assembly and the variable-area turbine-nozzle diaphragm were installed in the engine. Use of the mixer resulted in a substantial, though unexpected, improvement in the surge limit at high equivalent engine speeds. Because of the urgency of the surge program, an evaluation of the mixer effect was postponed; as a result, rather limited data were obtained for the original configuration (A1) without mixer.

[redacted]

A map of the compressor performance with the mixer (configuration A) is presented in figure 11 for operation at an altitude of 30,000 feet and a flight Mach number of 0.64. The compressor surge limit is given by the solid line. The change in slope of the surge line between 6740 and 7300 rpm is characteristic of high-pressure-ratio compressors. The fact that the weight flow is almost constant at speeds of 7310 and 7710 rpm indicates that the inlet stage of the compressor is approaching choked flow.

2616

Interstage performance. - The interstage pressure and temperature data obtained in the first, fourth, eighth, and eleventh stages were used to determine the performance curves for the first, middle, and rear sections of the standard compressor (configuration A). The data were arithmetically averaged across the passage and correlated by plotting the pressure coefficient T_iY/U_t^2 against the flow parameter $\frac{W_a\sqrt{\theta_i}/\delta_i}{U_t/\sqrt{\theta_i}}$, which is proportional to the ratio of volume flow based on stagnation density to tip speed at the inlet of each of the compressor sections. These curves are presented in figure 12 for the standard engine. The flow parameter is indicative of the reciprocal of the angle of attack. The interstage data were computed in this form in order to determine the region in the compressor which was instigating the high-speed surge problems in this particular compressor. The data of figure 12 indicate that increases in engine speed result in shifts in the operating points of the front and middle sections away from stall toward reduced angles of attack and therefore in increased values of the flow parameter. In the exit section of the compressor, however, increases in speed result in a shift in the point of operation toward the stall region, as evidenced by the decreasing flow parameter and increasing pressure coefficient. It appears, therefore, that the high-speed stall problems encountered in this compressor were the result of the stall in the exit stages.

The slightly positive slope of the high-flow end of the performance curve for the inlet section of the compressor is the result of an approaching choking condition in the inlet stage of the compressor. This choking condition is more clearly indicated in figure 13, in which the stage pressure coefficient is plotted against the flow parameter for the first, fourth, eighth, and eleventh stages. The data of figure 13 indicate that neither the first nor the fourth stages are seriously stalled for the range of speeds investigated, as evidenced by the fact that the pressure coefficients for these stages do not drop off at reduced values of flow parameter. The values of pressure coefficient for the inlet stage include the effect of losses in the ducting from the engine inlet to the compressor inlet. However, the extremely

low values of pressure coefficient at high speeds (in the vicinity of design speed) indicate the hub turbining condition. Thus, increasing the hub angle of attack is a requirement for improved operation of the inlet stage at high speeds. The eighth stage appears to be operating at approximately the same point for the entire range of conditions investigated. As has been pointed out in reference 5, this is to be expected of a stage in the rear half of an axial-flow compressor. It is this region of the compressor that should be highly loaded, because a wide range of operation is not required. The exit stage of the compressor operates similarly to the exit section presented in figure 12; that is, an increase in the engine speed results in a shift in the stage operating point towards the stall region. Thus, the surge problems at high speed are the result of stall in the exit stages.

2616

Although the interstage pressure and temperature data were arithmetically averaged along the radius for computation of the stage and section performance curves of figures 12 and 13, analysis of the radial distributions of the flow conditions within the compressor helps to point out specific regions of flow breakdown which are not indicated by the average stage curves. Typical total-pressure-ratio distributions at each of the interstage measuring stations are presented in figure 14 for an equivalent engine speed of 7198 rpm. Also shown for comparison are the design total-pressure-ratio distributions. In general, agreement between design and measured data was good. However, in the inlet stages, both the hub and tip sections produced less pressure rise than the design values. The low pressure ratios at these sections were probably the result of the high angles of attack computed at the tip section of the first rotor and the low angles at the hub section. The greater effect is that of the low hub angles of attack as indicated by the greater difference between design and actual pressure ratios at the hub sections. The experimental pressure ratios include the friction pressure drop in the inlet duct ahead of the compressor. This pressure loss varies from $\frac{1}{2}$ to $1\frac{1}{2}$ percent of the engine-inlet total pressure and effects a reduction in measured pressure ratio of approximately the same magnitude. The effect of the boundary-layer growth along the walls of the double inlet duct on the angles of attack and pressure rise of the inlet stages cannot be accurately evaluated because of the lack of data on the extent of the boundary-layer growth.

As is indicated in figure 14, the hub sections of the seventh and eighth stages appear to be stalled out, probably as a result of the poor flow conditions at the hub of the inlet stages. Although the hub sections of the seventh and eighth stages are stalled, pressure conditions at the exit of the tenth stage satisfy design requirements almost exactly. The indication is, therefore, that between the eighth and tenth stages, the hub stall region is eliminated and flow conditions

recover to the design values. Similar results have been noted in other investigations, which indicate that poor flow conditions set up in several stages of a conservatively designed multistage compressor may be smoothed out in later stages so as to give a satisfactory distribution at the compressor discharge.

2616

Effect of Blade Modifications on Surge Line

The effect of modifying the original XJ40-WE-6 compressor, by blade-angle adjustments, on the position of the surge line is indicated in figures 15 and 16 by curves of compressor pressure ratio at its surge points against equivalent engine speed. The data of figure 15 show the flat portion of the surge-limit curve which was also characteristic of the compressor without mixer. Although this configuration indicated an effect of altitude on the surge limit, the other configurations showed no consistent altitude effect within the accuracy of the experimental data. The surge lines for the different compressor configurations are superimposed in figure 16.

The surge line for the standard compressor with mixer (configuration A) is seen to level off rapidly at a speed of approximately 7400 rpm and then increase only slightly up to the maximum speed investigated (8000 rpm). When the tips of the ninth and eleventh rotors were closed by 3° and 6° respectively (configuration B), there resulted a noticeable drop in the surge limit over the entire speed range. The analysis of reference 5 and previous experimental results indicated that unloading the exit stages of a compressor would result in a decrease in surge-point pressure ratio at any given engine speed below the design speed. Along with this decrease in pressure ratio, these results indicated a decrease in weight flow, which causes the position of the surge line to be almost unaffected on a pressure-ratio against weight-flow curve. The engine data obtained indicated that the weight flow was actually reduced for configuration B at speeds below design speed. Although application of the analysis of reference 5 indicated that unloading the exit stages should increase the surge pressure ratio at speeds above design, the fact that the pressure ratio was slightly reduced by this modification in the high-speed operating range indicated that the tip sections of the exit stages were not operating critically in the original compressor. Because high-speed surge is the result of stalling in the exit stages, it appears that the hub sections of the exit stages were the critical sections which were stalling at the speeds above design. This conclusion was also corroborated by preliminary data obtained in the initial runs of the engine.

In an attempt to unload the hub sections of the exit stages, the stator blades of stages 7 to 10 were closed by 3° (configuration C).

On the basis of the results of the stage-matching analysis of reference 5 and experimental results, it was expected that such a modification would have a detrimental effect on the surge condition below design speed but that an improvement would result at speeds above design. The actual result is indicated in figure 16. The pressure ratio at surge was reduced appreciably at speeds below 7650 rpm, but the surge pressure ratio increased continuously with speed and did not level off at the high speeds. Thus, unloading the hub sections resulted in a definite improvement in the general shape of the surge line; but the large reduction in pressure ratio at speeds below 7650 rpm might instigate acceleration and take-off problems.

2616

Therefore, a shift in the surge line to increased pressure ratio at a given operating speed is required in order to achieve satisfactory stable operation over the entire range of engine speeds. As has been discussed in the Compressor Design Analysis section, the design of the first three stages of the compressor neglected the requirement of radial equilibrium. As a result, the angle of attack at the tip of the first-stage rotor was approximately 10° higher than design, and the hub angle was 4° lower than design. The extremely high angle of attack at the tip would be expected to cause the inlet stages of the compressor to stall at a comparatively high speed. Thus, improvement in flow conditions in the inlet stages of the compressor to approach more nearly those conditions required to satisfy radial equilibrium should result in a noticeable improvement in the compressor surge characteristics, especially at speeds below design. The blade adjustments of configuration D were directed toward satisfying this objective. The adjustments did not, however, alter flow conditions at the first rotor hub section. The effect of this modification on the surge-line pressure ratio is shown in figure 16 to be large at all equivalent speeds between 5400 and 7800 rpm. The surge curve of configuration C is shifted to higher values of pressure ratio at any given speed within this range by the adjustments in the blade angles in configuration D. In the high-speed range which was causing the difficulties in the operation of the original engine, the surge pressure ratio has been increased appreciably.

The fact that the surge pressure ratio remained almost constant for configurations C and D at speeds below 5400 rpm may be explained by considering the performance of the inlet stage of the compressor. As is indicated by the performance curves for the highly cambered single stage with modified guide vanes presented in reference 6 and by the single-stage curve presented in reference 5, the stage pressure ratio remains essentially constant at the low flows or high rotor angles of attack. This fact is the result of a tip stall condition which causes a recirculating flow at the tip of the first rotor and a displacement of the flow inward. The increased flow at the hub section

of the rotor permits this section of the blade row to operate at satisfactory angles of attack and reasonable pressure ratios. The fact that the tip section has practically no through-flow velocity component (all of the velocity is recirculatory) results in a constant value of mass-averaged pressure ratio as the weight flow is reduced. Such a phenomenon was believed to exist in the present compressor. Therefore, it appeared that the inlet stages of the present compressor were operating on the flat portion of the stage-pressure-ratio curve at speeds below 5200 rpm for both configurations C and D, so that the change in the surge line below this speed is negligible.

2616

Because the blade adjustments of configuration B resulted in a reduced surge pressure ratio from that obtained for the original compressor, it was decided to twist the ninth and eleventh rotor blades back to their original angle setting. The effect of this configuration E, as shown in figure 16, is small but in the desired direction for equivalent engine speeds over 6600 rpm.

Comparison of the surge line for configuration A with that obtained by configuration E indicated a decrease in pressure ratio over the range of speeds below 7500 rpm with a noticeable improvement achieved at speeds above 7500 rpm.

Effect of Mixer on Surge Limit

Inasmuch as configuration E appeared to be the best possible solution to the compressor surge problem without major compressor rework, it was decided to evaluate the performance of the engine with a production-turbine diaphragm, and with the mixer replaced by the standard outlet guide vane (configuration E1). The latter step was taken because of difficulties in obtaining rapid production of mixer assemblies. As shown by the data of figure 17, the surge limit was reduced markedly at high equivalent engine speeds when the mixer was removed and the standard turbine nozzle installed. For example, at a corrected speed of 7800 rpm the surge limit was reduced from about 5.68 to 5.41. This unexpected result led to the conjecture that a difference in the radial variation in flow resistance afforded by the mixer as compared with the standard outlet vane assembly might redistribute the flow in the latter compressor stages. Accordingly the total-pressure profiles at the inlet and outlet of both assemblies were compared; however, the differences noted appeared to be too small to be considered a suitable explanation. To verify this effect of the mixer, it was reinstalled (configuration E2) and the surge limit was again raised. This same result was obtained with configuration A; however, it may be noted by comparing figures 16 and 17 that the effect of the mixer on the surge limit was slightly greater for configuration E than for configuration A.

2616

Effects of Compressor Modifications on Performance

The merits of the various compressor configurations cannot be properly evaluated without consideration of the effects of the modifications on over-all engine performance. Accordingly, the effects of these modifications on air flow, compressor efficiency, and surge pressure ratio are summarized in the following table for operation at an altitude of 30,000 feet and a flight Mach number of 0.64, which corresponds to an equivalent engine speed of 7830 rpm:

Modification	Air flow	Compressor adiabatic efficiency	Surge pressure ratio
A1	143.9	0.755	5.4*
A	144.2	.766	5.58
B	143.6	.758	5.51
C	144.3	.768	5.65
D	141.8	.758	5.66
E	142.3	.763	5.68
E1	*	*	5.41
E2	141.5	.763	5.68

*These values were not accurately established.

It is apparent from a comparison of the results of configuration A1 (the original engine as received) and A (the standard engine with the mixer and the variable-area turbine nozzle installed) that the effect of the mixer was to increase the efficiency and the high-speed surge pressure ratio of the compressor. The exact magnitudes of the increase were not determined, because only meager data were obtained for the original engine configuration. In addition to a reduction in the high-speed surge pressure ratio, configuration B (unloading the tips of the ninth and eleventh rotors) caused a slight decrease in compressor efficiency. Configuration C resulted in an appreciable improvement in the high-speed surge pressure ratio but, as mentioned earlier, had a detrimental effect on the lower speed performance. As was expected, configuration D caused a decrease in the high-speed weight flow and efficiency. It is to be expected that if the hub section of the first rotor had been loaded by either guide-vane adjustment or rotor resetting, then the performance at high speed would probably have remained the same as for the C configuration. The effect of twisting the ninth and eleventh rotor tips back to their original settings (configuration E) was as expected: the surge pressure ratio and the efficiency were increased slightly.

The effect of the mixer on the surge limit is again demonstrated by comparison of configuration E and E1. Although instrument icing conditions prevented the determination of complete and accurate weight-flow data for configuration E1, it is apparent that the surge pressure ratio was decreased appreciably as was the compressor efficiency when the mixer was removed.

2616

The over-all effect of the modifications made to the compressor is indicated in figure 18, where curves of the ratios of both calculated net thrust (appendix B) and measured weight flow for the final configuration with mixer (E and E2) and the original compressor without mixer (A1) are presented as a function of equivalent engine speed. A single curve was faired through the data of configurations E and E2. These data are for operation at an altitude of 30,000 feet and a flight Mach number of 0.64; however, because the Reynolds number effects are small below 35,000 feet, these data may be considered to apply at sea-level conditions as well. It will be noted that the air flow of configuration E was less than that of the original configuration for the range of speeds investigated. As a result, the thrust was also lower at equivalent engine speeds below the approximate value at which the original compressor became surge limited. At equivalent speeds above 7680 rpm, the thrust of the original engine was lower than that of configuration E because of the influence of the surge limit.

CONCLUDING REMARKS

As a result of the investigation reported herein, it was shown that slight improvements in the compressor surge limit and the operation margin were possible by making minor, easily incorporated changes in the compressor. However, some of the changes also reduced engine air flow and hence reduced the thrust. It was also found that the use of a mixer at the compressor outlet improved the surge limit with no appreciable thrust penalty.

Lewis Flight Propulsion Laboratory
National Advisory Committee for Aeronautics
Cleveland, Ohio

2616

APPENDIX A

SYMBOLS

The following symbols are used in this report:

$c_{p,a}$	specific heat of air, 0.24 Btu/(lb)($^{\circ}$F)
$c_{p,g}$	specific heat of exhaust gas, Btu/(lb)($^{\circ}$F)
F_n	net thrust, lb
f/a	fuel-air ratio
g	gravitational constant, 32.2 ft/sec^2
K,K'	constants
N	engine rotational speed, rpm
$N/\sqrt{\theta}$	sea-level equivalent speed, rpm
P	total pressure, lb/sq ft abs
p_0	ambient altitude pressure, lb/sq ft abs
r	radius, in.
T	total temperature, $^{\circ}$R
T/θ	sea-level equivalent total temperature, $^{\circ}$R
U	blade speed, ft/sec
$V_{j,eff}$	effective jet velocity, ft/sec
V_z	axial velocity, ft/sec
V_0	flight speed, ft/sec

W_a air weight flow, lb/sec

$W_a\sqrt{\theta}/\delta$ sea-level equivalent weight flow, lb/sec

W_g exhaust-gas weight flow, $W_a(1 + f/a)$, lb/sec

Y pressure function $\left[\left(\frac{P_o}{P_i}\right)^{\frac{\gamma-1}{\gamma}} - 1\right]$

α angle of attack, deg

γ isentropic exponent

γ_a ratio of specific heats for air

γ_g ratio of specific heats for exhaust gas

Δh_c enthalpy rise through compressor, Btu/lb

Δh_t enthalpy drop through turbine, Btu/lb

δ ratio of total pressure to standard sea-level pressure

η_c compressor adiabatic efficiency

η_t turbine adiabatic efficiency

θ ratio of total temperature to standard sea-level temperature

Subscripts:

a air

c compressor

g exhaust gas

i inlet of stage or section

j jet

2G192

[redacted]

n	net
o	outlet of stage or section
t	rotor tip section, turbine
0	ambient
1	cowl inlet
2	engine inlet
3	compressor inlet
4	compressor discharge
5	turbine inlet
6	turbine outlet
7	exhaust nozzle

2616

2616

APPENDIX B

CALCULATION OF IDEAL NET THRUST

During initial performance tests of the original configuration, unexpected compressor surge at high equivalent engine speeds resulted in minor damage to the tunnel scales. Hence the thrust readings could not be considered reliable. In later tests of other compressor configurations, thrust data were not obtained at rated performance because limiting turbine-inlet temperatures could not be maintained.

In order to compare impartially the performance of various configurations at rated conditions it was necessary to rely on calculated values of net thrust. Although the magnitude of such calculated thrusts may be in error, the use of ratios for a comparison is probably reliable.

The ideal net thrusts of the original and final compressor configurations, which are presented in figure 18 as a ratio, were obtained by the following method of calculation.

When choked flow through the turbine nozzle is assumed for equivalent engine speeds greater than 7000 rpm, the continuity equation may be used to obtain the following relation:

$$\frac{\frac{W_a\sqrt{\theta}}{\delta}\sqrt{\frac{T_5}{\theta}}}{\frac{P_5}{P_2}} = K' \qquad (1)$$

If the pressure drop through the combustion chamber is considered constant, equation (1) may be expressed in terms of equivalent air weight flow, turbine-inlet temperature, and compressor pressure ratio as

$$\frac{\frac{W_a\sqrt{\theta}}{\delta}\sqrt{\frac{T_5}{\theta}}}{\frac{P_4}{P_2}} = K \qquad (2)$$

Since engine performance is evaluated from station 2 (engine inlet), the compressor pressure ratio is considered to be from station 2 to station 4.

An average value of the constant K was determined from experimental data obtained at several high equivalent engine speeds. At actual rated engine speed N of 7260 rpm, θ was calculated for equivalent engine speeds $N/\sqrt{\theta}$ of 7000, 7200, 7400, 7600, 7800, and 8000 rpm. Values of equivalent weight flow $W_a\sqrt{\theta}/\delta$ at the above equivalent engine speeds were obtained from faired curves of experimental data. The turbine-inlet temperature T_5 was assumed limiting at 1885 °R (manufacturers' specification), and the compressor pressure ratio P_4/P_2 was calculated from equation (2).

2616

When the pressure ratio is known, the enthalpy rise, which is the actual work of compression per unit weight flow, may be calculated from

$$\Delta h_c = \frac{c_{p,a} T_2 \left[\left(\frac{P_4}{P_2} \right)^{\frac{\gamma_a - 1}{\gamma_a}} - 1 \right]}{\eta_c} \tag{3}$$

where compressor efficiency η_c is obtained from experimental data.

When the enthalpy rise across compressor is assumed equal to the enthalpy drop across turbine, the turbine-outlet temperature T_6 may be calculated from

$$\Delta h_c = \Delta h_t = \frac{W_g}{W_a} c_{p,g} (T_5 - T_6) \tag{4}$$

where $W_g/W_a = (1 + f/a)$, and the fuel-air ratio is assumed equal to 0.015.

The turbine-outlet total pressure P_6 may then be calculated as follows:

$$P_6 = P_5 \left[1 - \frac{\left(1 - \frac{T_6}{T_5} \right)}{\eta_t} \right]^{\frac{\gamma_g}{\gamma_g - 1}} \tag{5}$$

2916

where the turbine efficiency η_t is obtained from experimental data, and the turbine-inlet total pressure P_5 is assumed to be 95 percent of compressor-discharge total pressure. From P_6 the effective jet velocity $V_{j,eff}$ was calculated for full expansion to ambient altitude pressure p_0 (628 lb/sq ft abs at 30,000 ft) for a γ_g of 1.3.

Actual weight flow W_a was calculated from the equivalent weight flow $W_a\sqrt{\theta}/\delta$, where δ corresponds to engine-inlet conditions at a flight Mach number of 0.64 at an altitude of 30,000 feet; and θ was determined at an actual engine speed of 7260 rpm for equivalent engine speeds of 7000, 7200, 7400, 7600, 7800, and 8000 rpm.

The net thrust was then calculated by subtracting inlet momentum from the jet thrust

$$F_n = \frac{W_g V_{j,eff}}{g} - \frac{W_a V_0}{g}$$

[redacted]

REFERENCES

1. Allen, Sydney, and Hamm, J. R.: A Pyrometer for Measuring Total Temperature in Low-Density Gas Streams. A.S.M.E. Trans., vol. 72, no. 6, Aug. 1950, pp. 851-858.

2. Delio, Gene J., and Schwent, Glennon V.: Instrumentation for Recording Transient Performance of Gas-Turbine Engines and Control Systems. NACA RM E51D27, 1951.

3. Finger, Harold B., Schum, Harold J., and Buckner, Howard A., Jr.: Experimental and Theoretical Distribution of Flow Produced by Inlet Guide Vanes of an Axial-Flow Compressor. NACA TN 1954, 1949.

4. Burtt, Jack R.: Investigation of Performance of Typical Inlet Stage of Multistage Axial-Flow Compressor. NACA RM E9E13, 1949.

5. Finger, Harold B., and Dugan, James F., Jr.: Analysis of Stage Matching and Off-Design Performance of Multistage Axial-Flow Compressors. NACA RM E52D07, 1952.

6. Jackson, Robert J.: Effects on the Weight-Flow Range and Efficiency of a Typical Axial-Flow Compressor Inlet Stage That Result From the Use of Decreased Blade Camber or Decreased Guide-Vane Turning. NACA RM E52G02, 1952.

2616

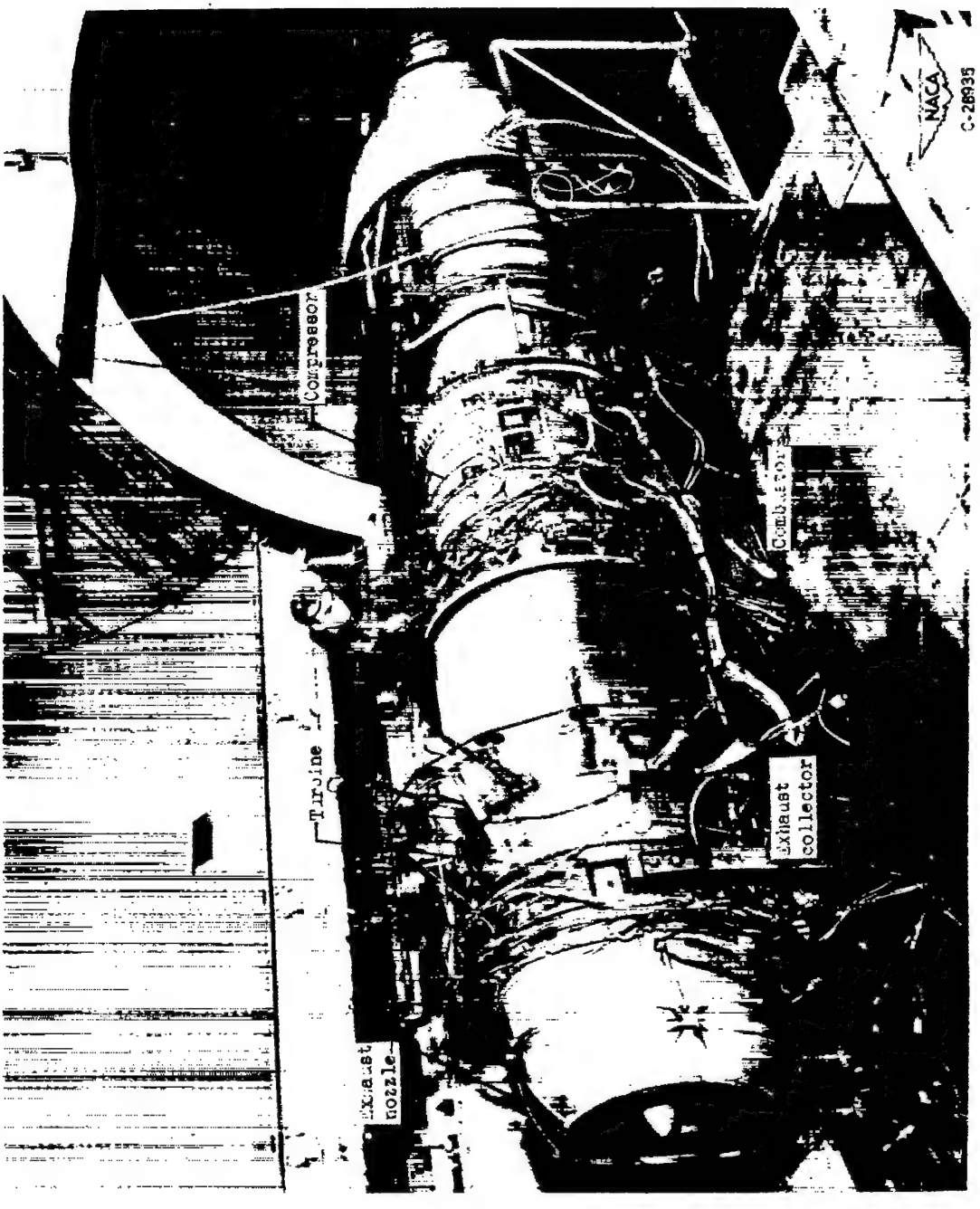

Figure 1. - KJ40-WE-6 engine installed in altitude wind tunnel.

2616

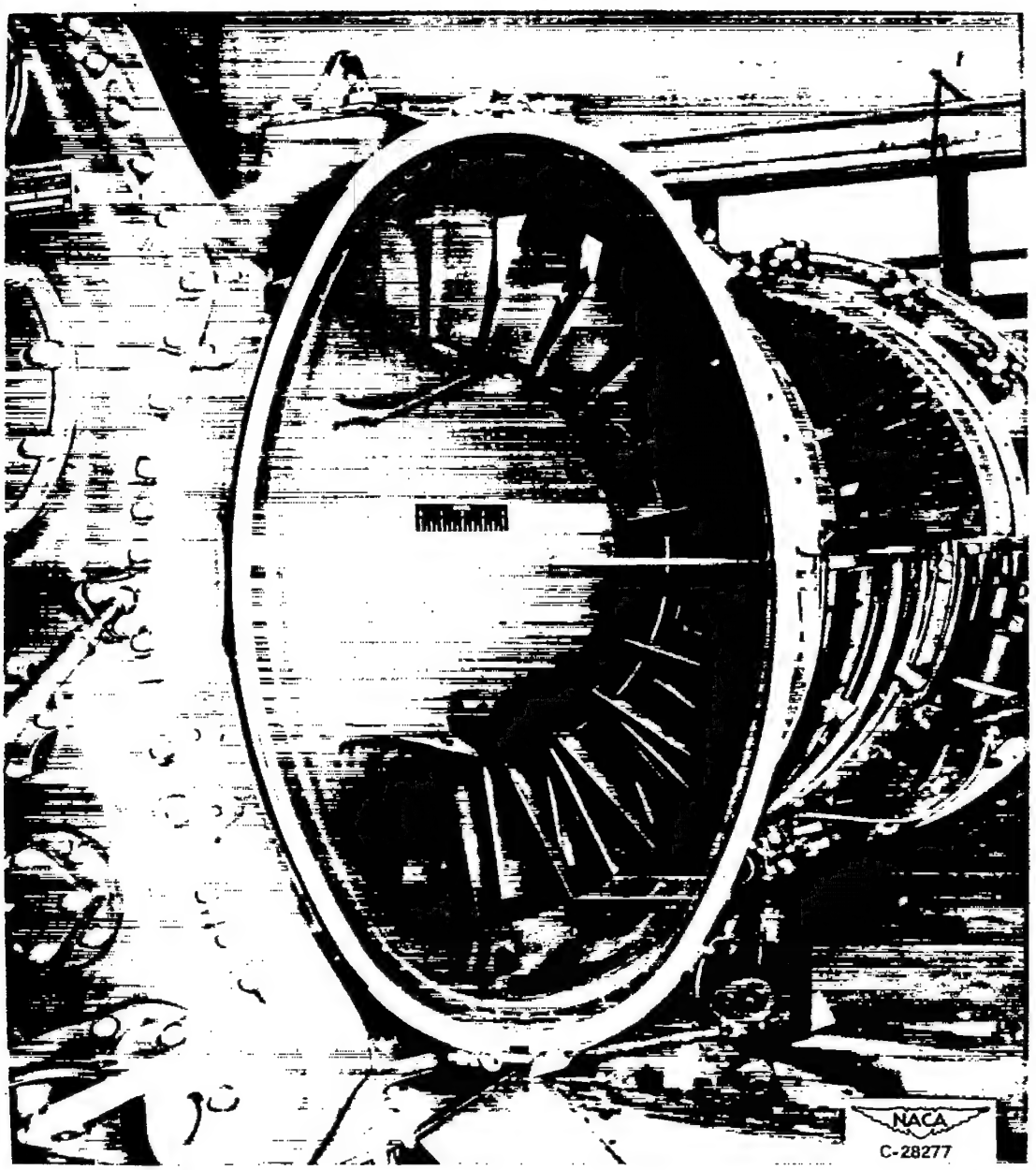

Figure 2. - Compressor-inlet duct section.

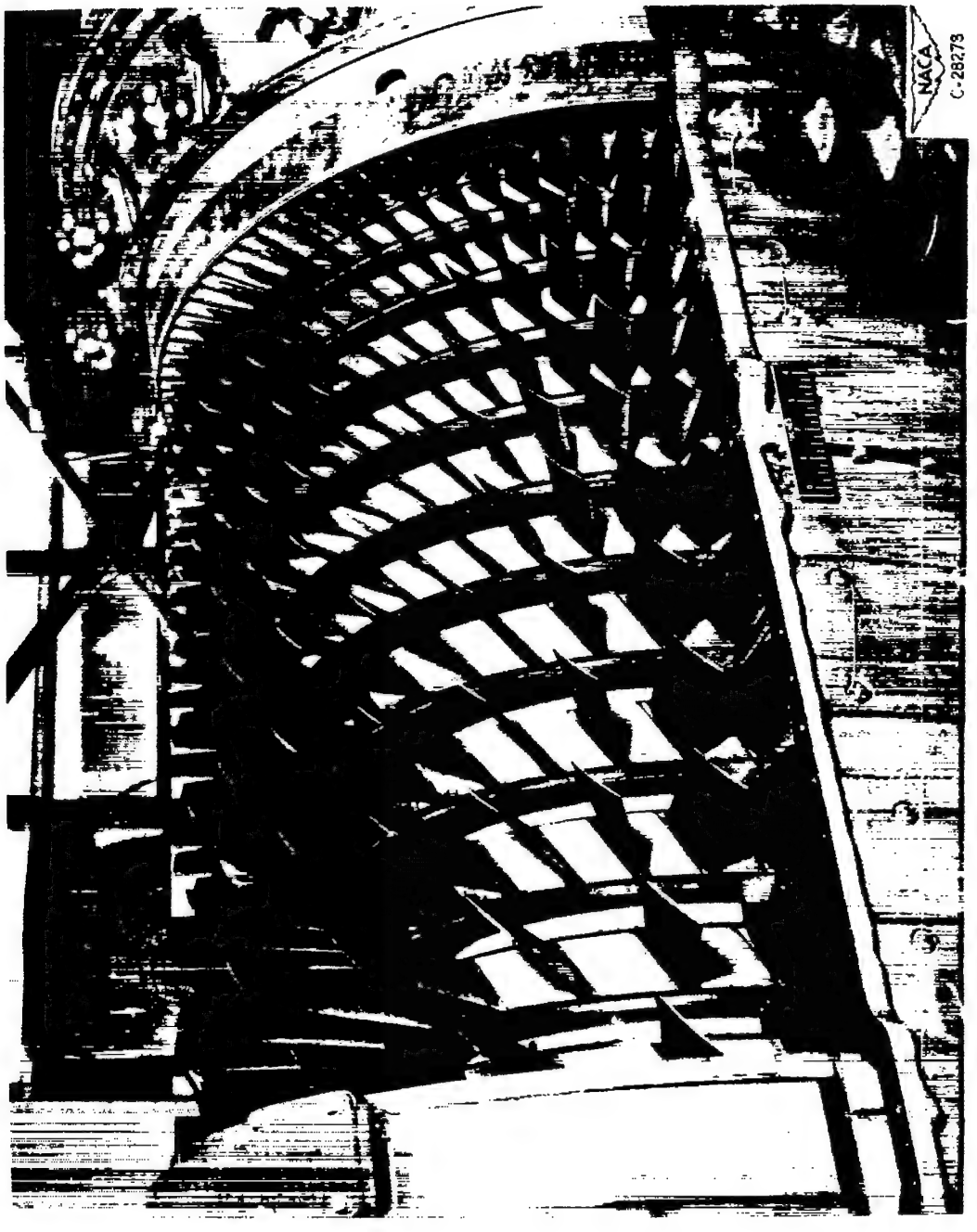

Figure 3. - View of compressor with top half of casing removed.

2616

2616

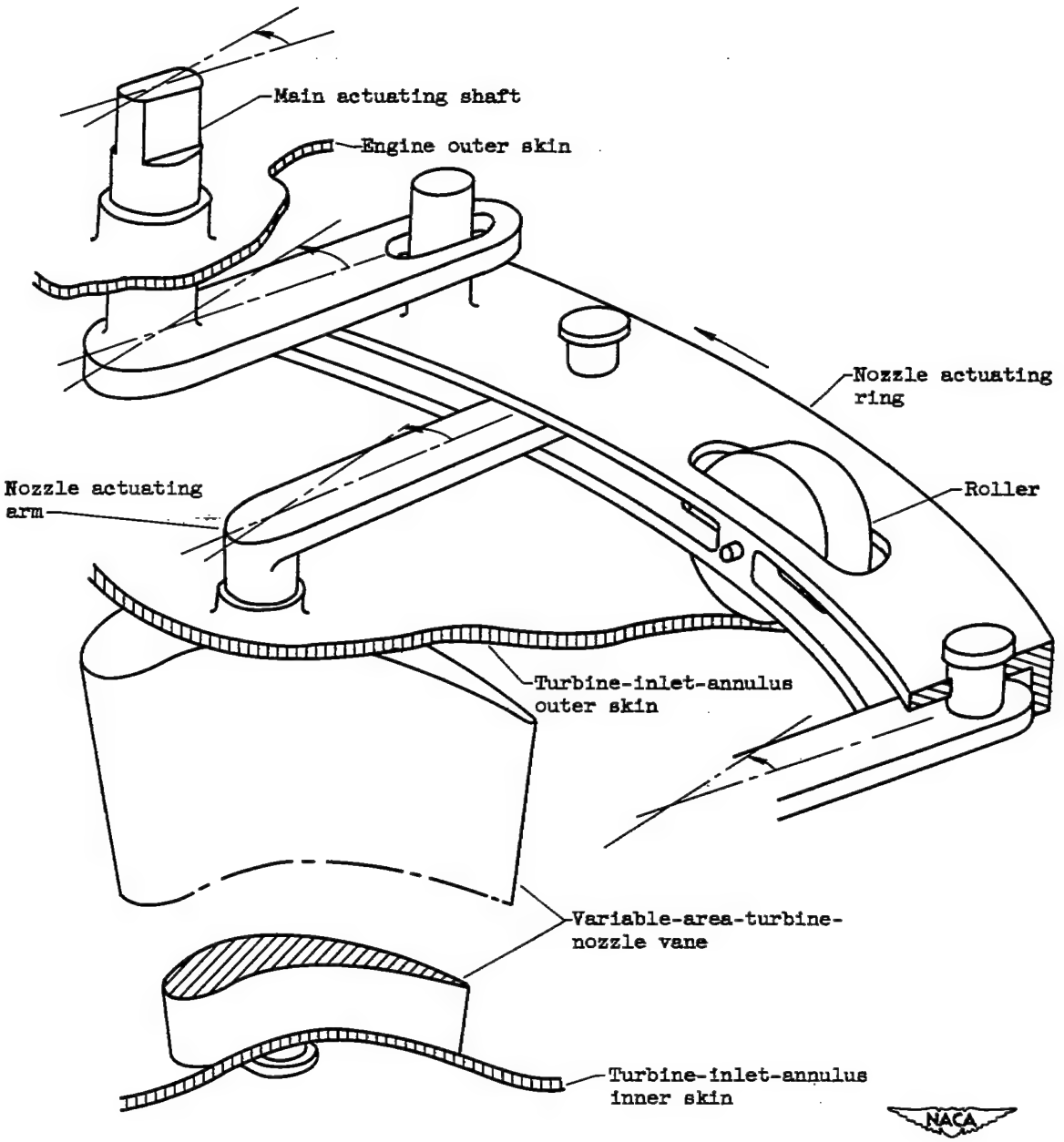

Figure 4. - Schematic sketch of variable-area-turbine-nozzle actuating mechanism.

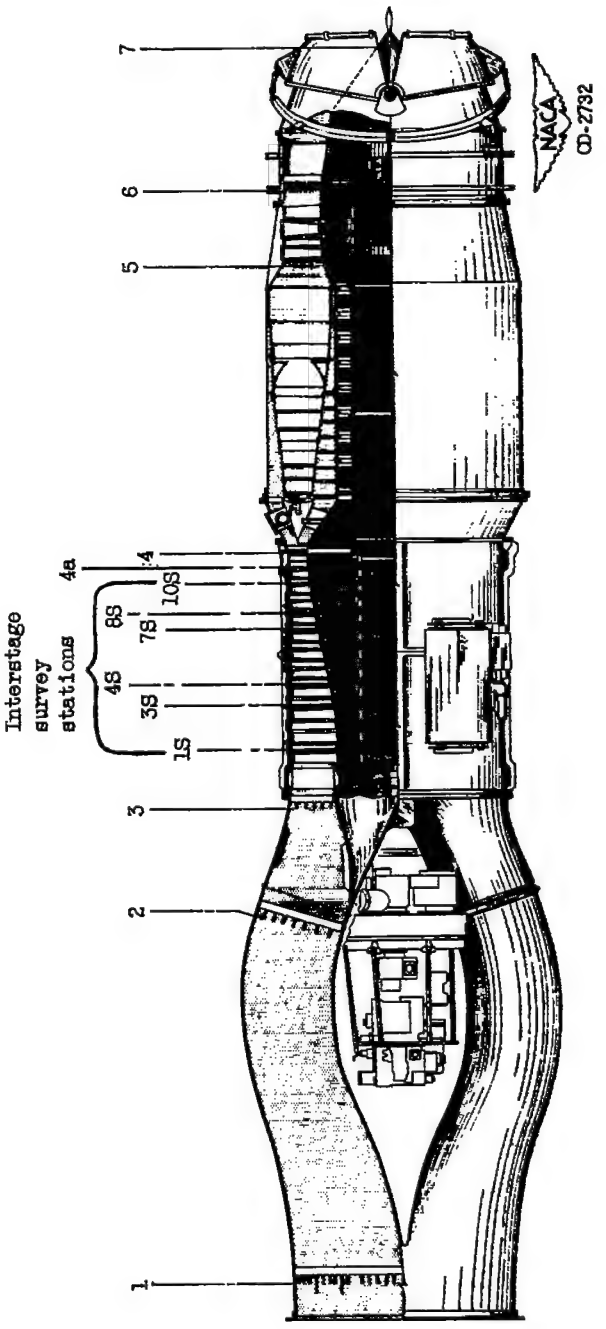

Figure 5. - Cross-section drawing of engine showing instrument stations.

9T92

2616

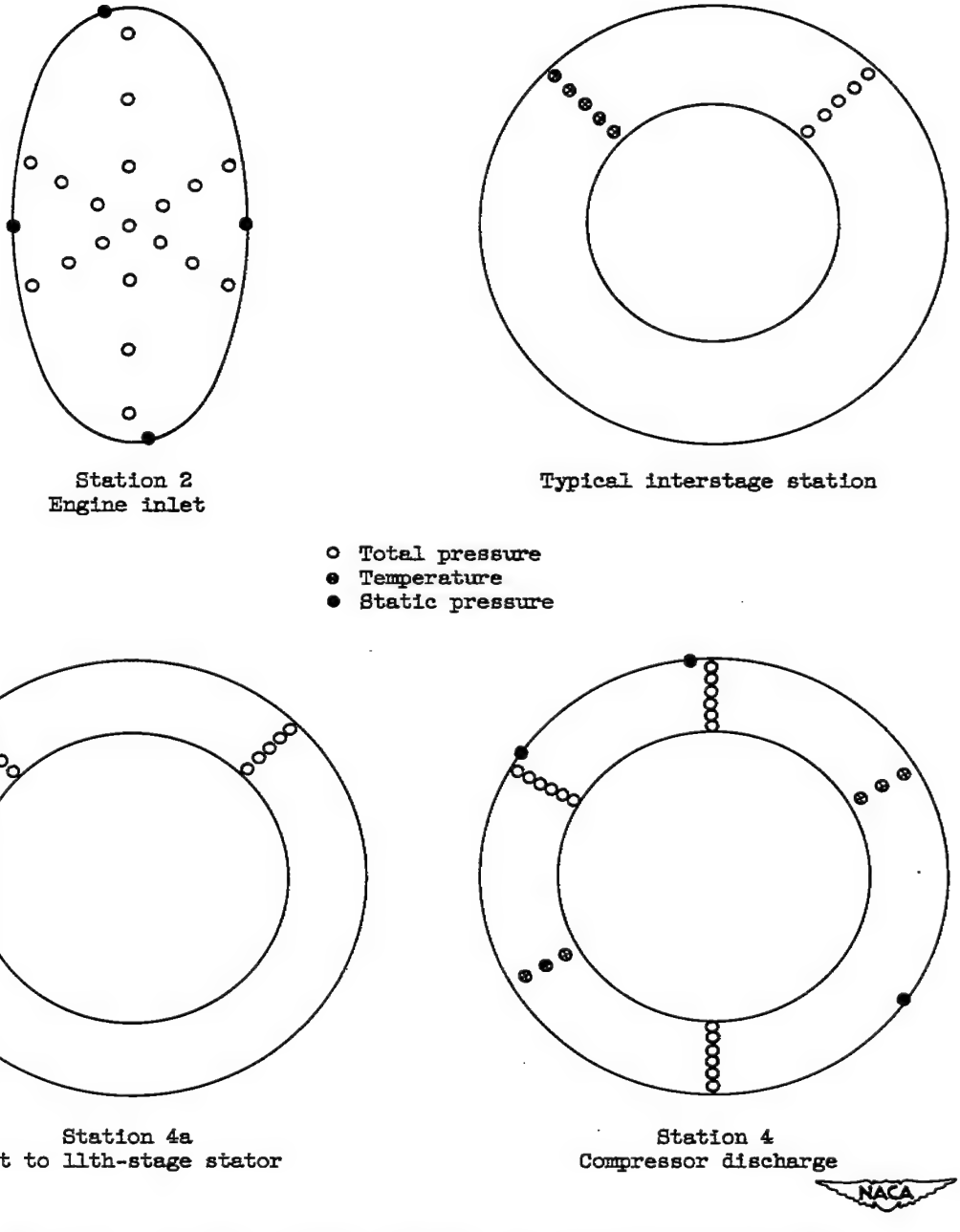

Figure 6. - Schematic diagram showing location of instrumentation at several compressor stations.

2616

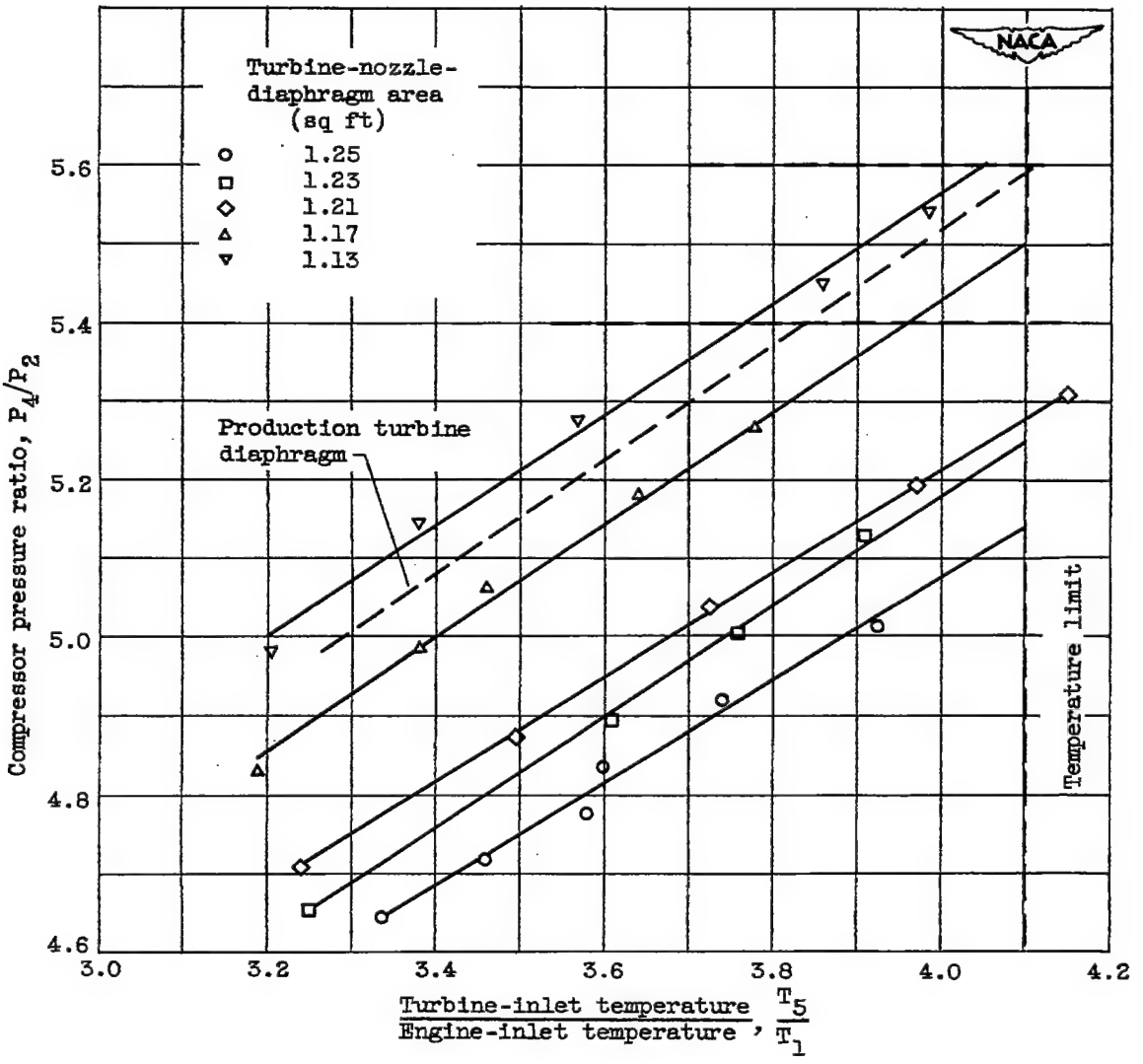

Figure 7. - Effect of changing area of turbine-nozzle diaphragm on compressor pressure ratio. Altitude, 30,000 feet; flight Mach number 0.64; equivalent engine speed $N/\sqrt{\theta}$ of 7710 rpm.

2616

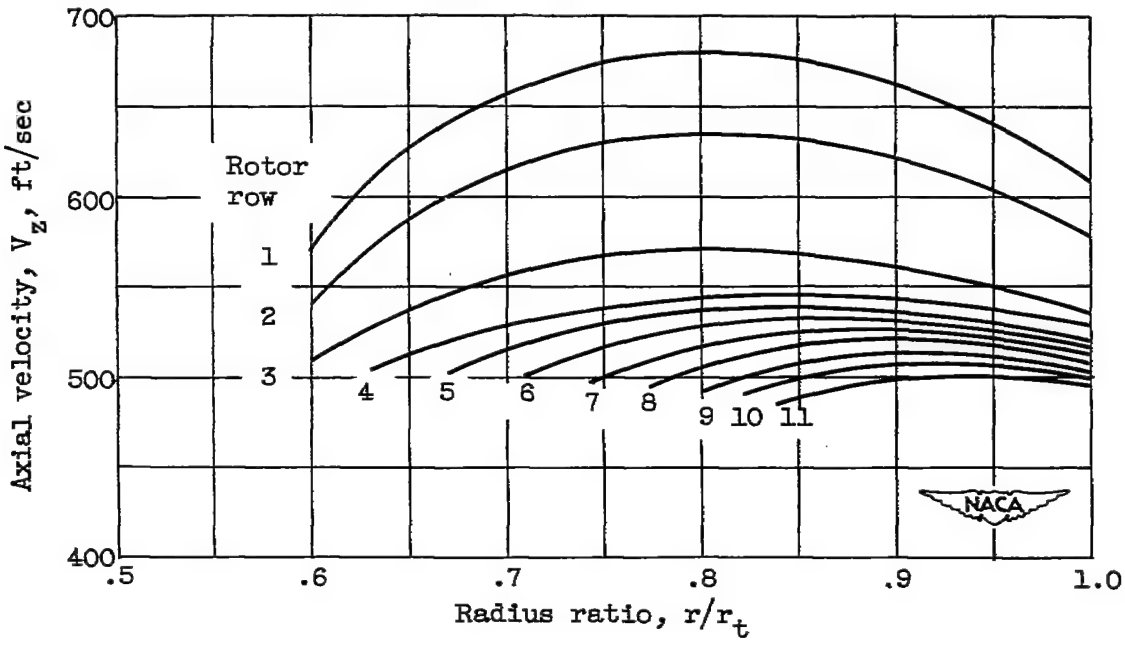

Figure 8. - Design axial-velocity distribution at rotor inlet on XJ40-WE-6 compressor.

[redacted]

2616

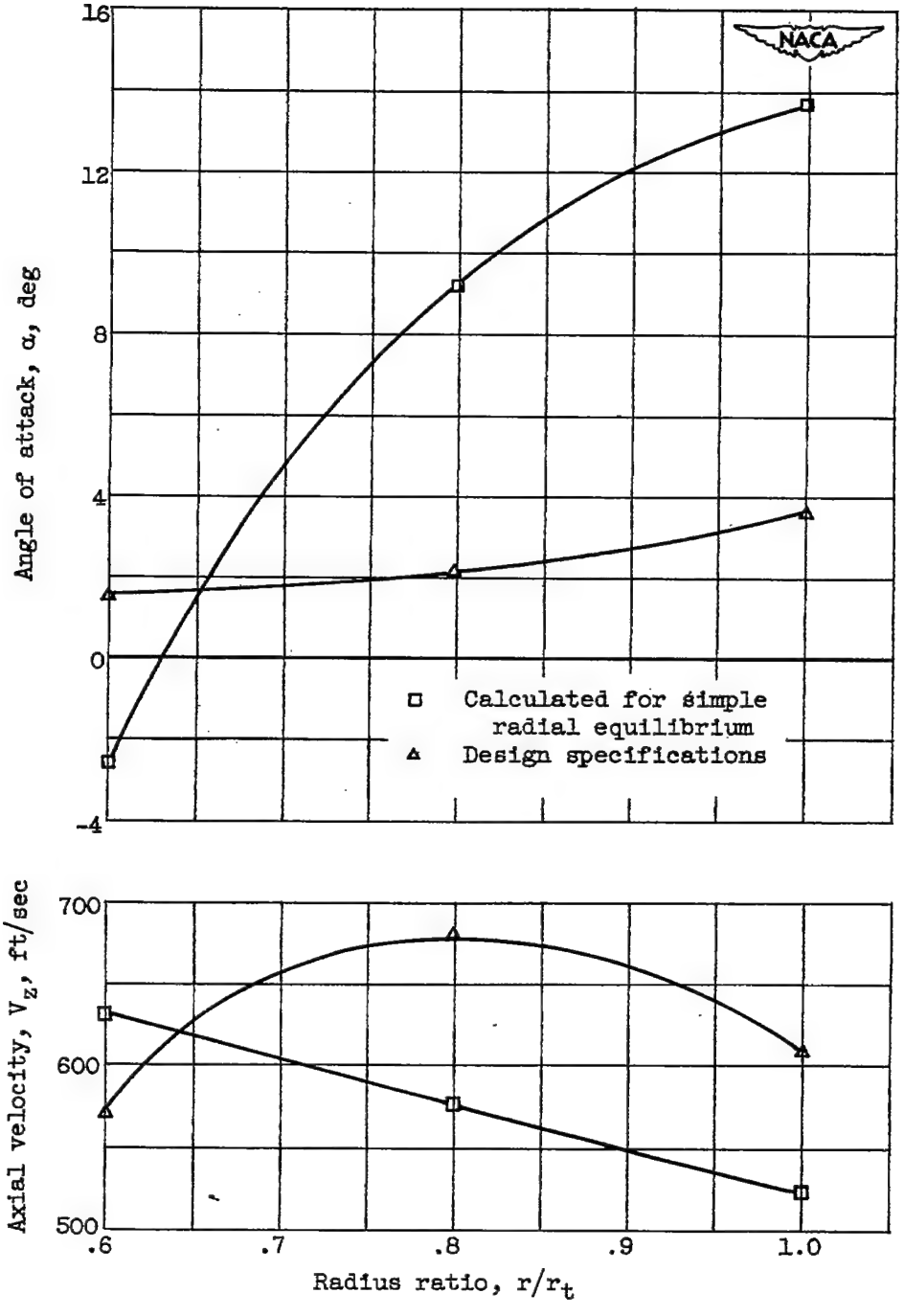

Figure 9. - Flow conditions at first rotor inlet for XJ40-WE-6 compressor.

2616

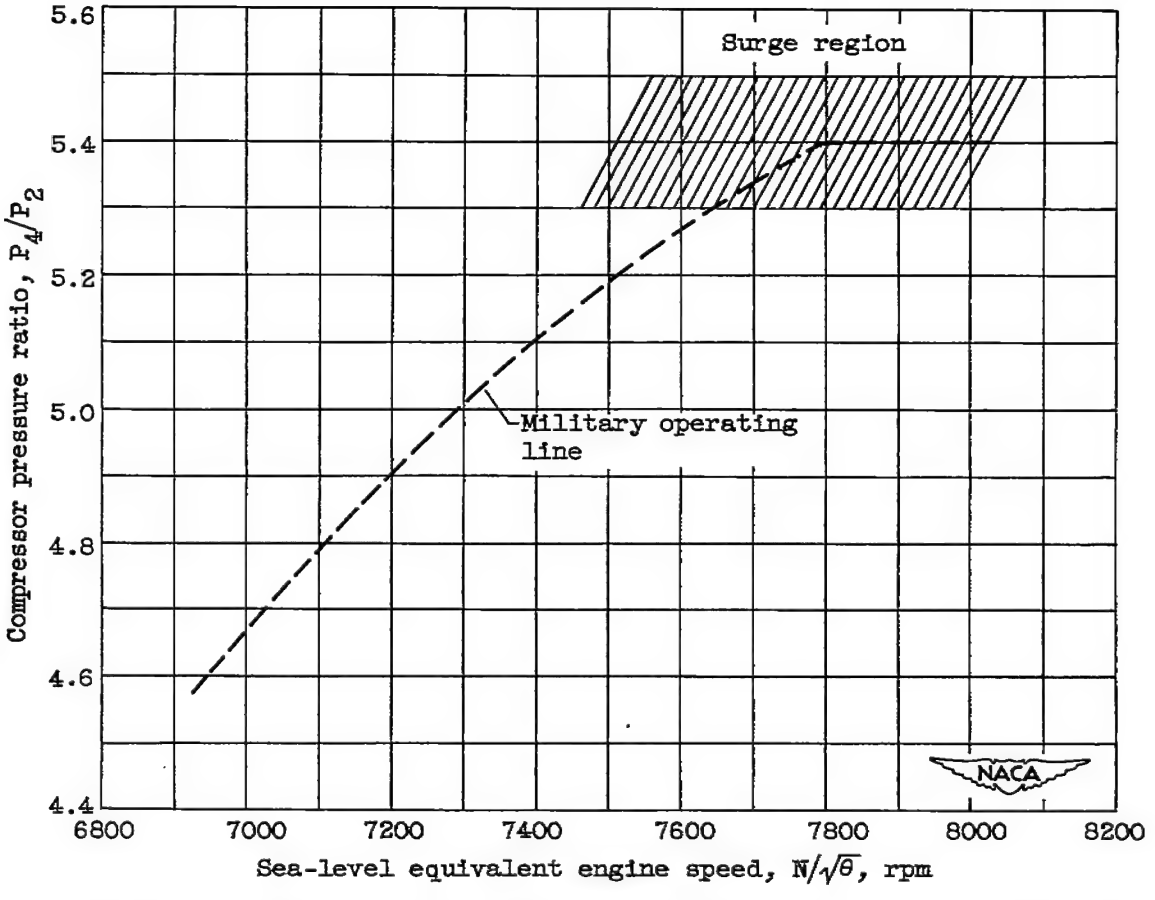

Figure 10. - Relation of military power operating line and surge limit of original compressor configuration (A1).

2616

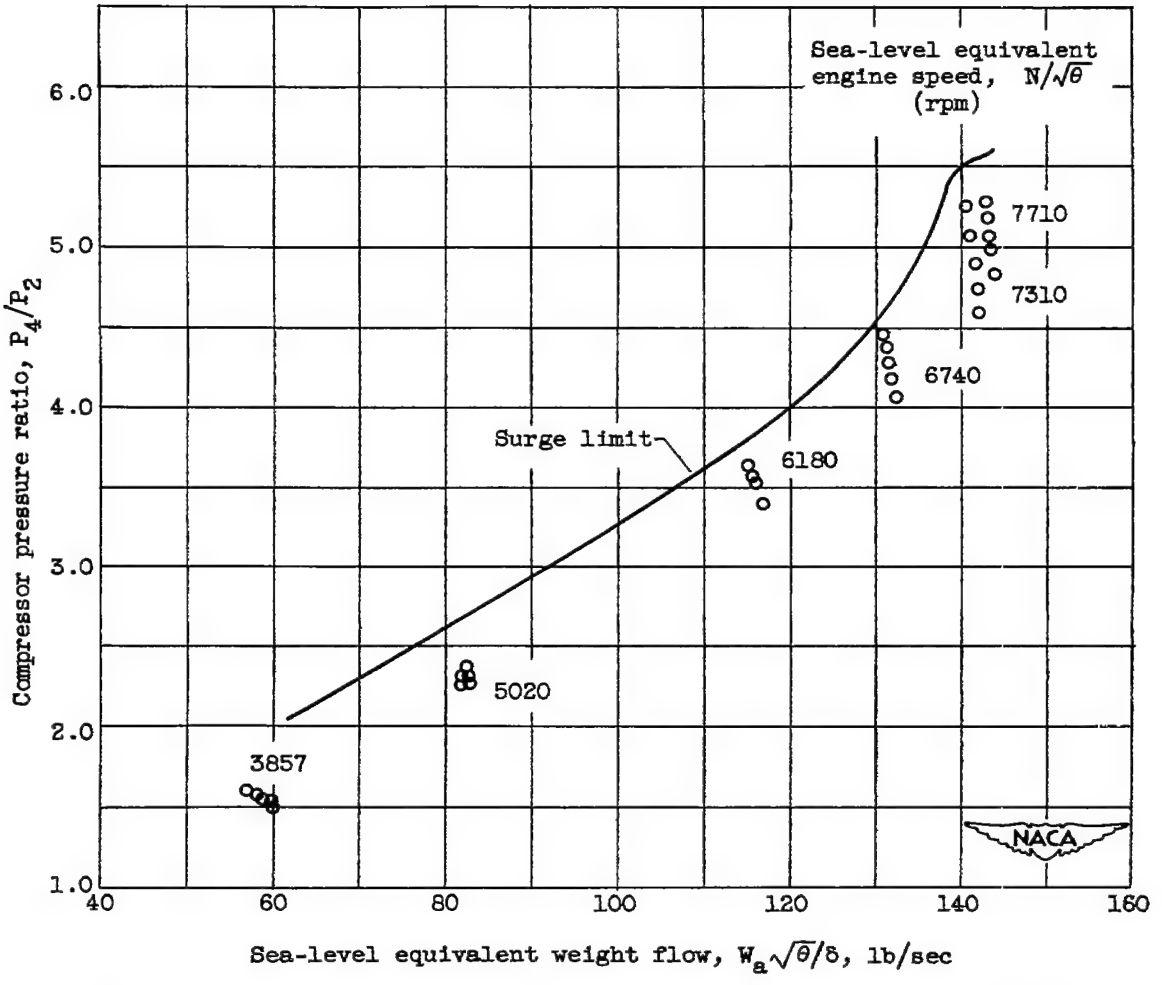

Figure 11. - Operating map of standard compressor with mixer installed (configuration A). Altitude, 30,000 feet; flight Mach number, 0.64.

2616

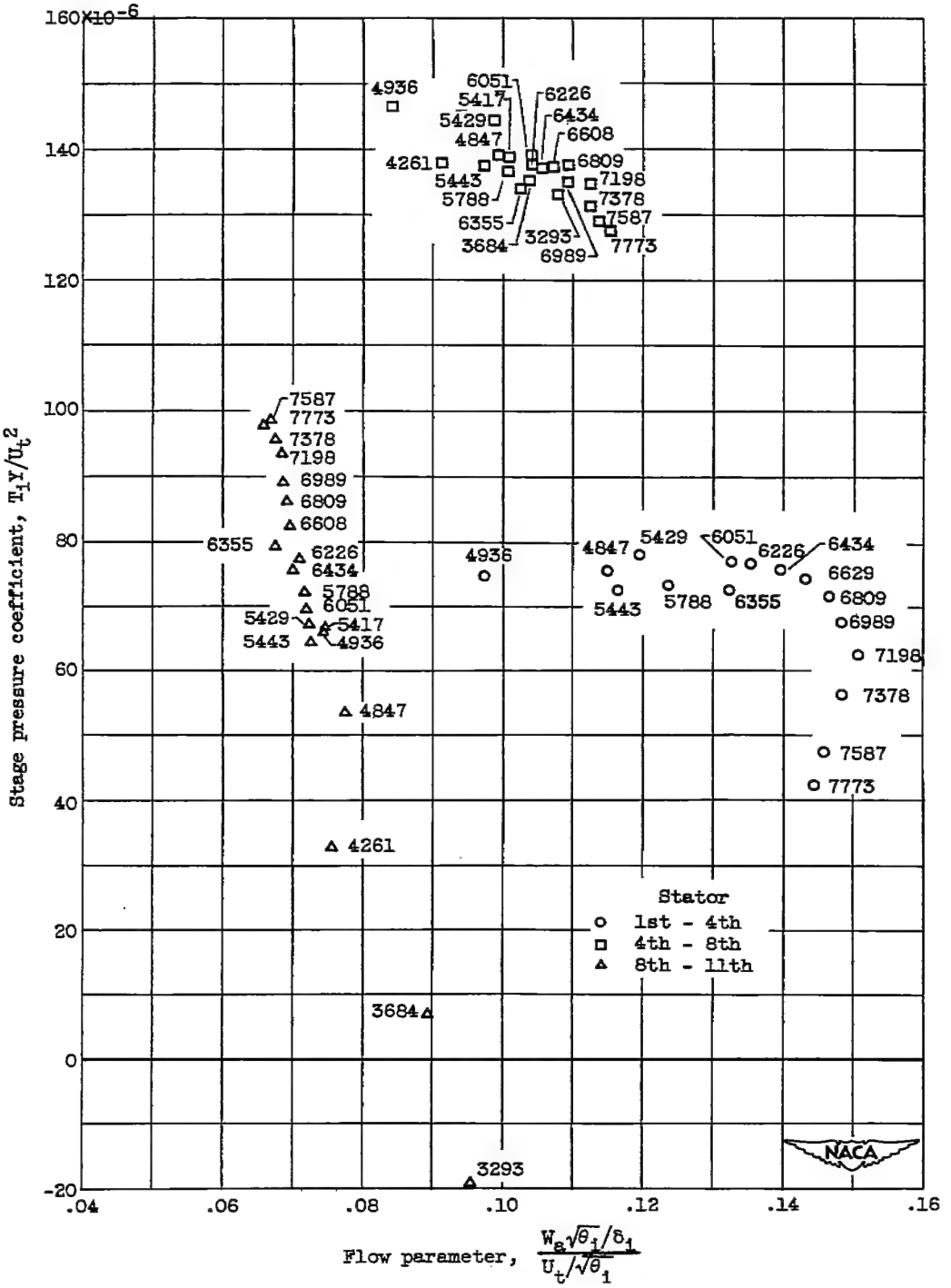

Figure 12. Operating points of front, middle, and rear sections of standard XJ40-WE-6 compressor for various equivalent engine speeds in rpm.

[redacted]

2616

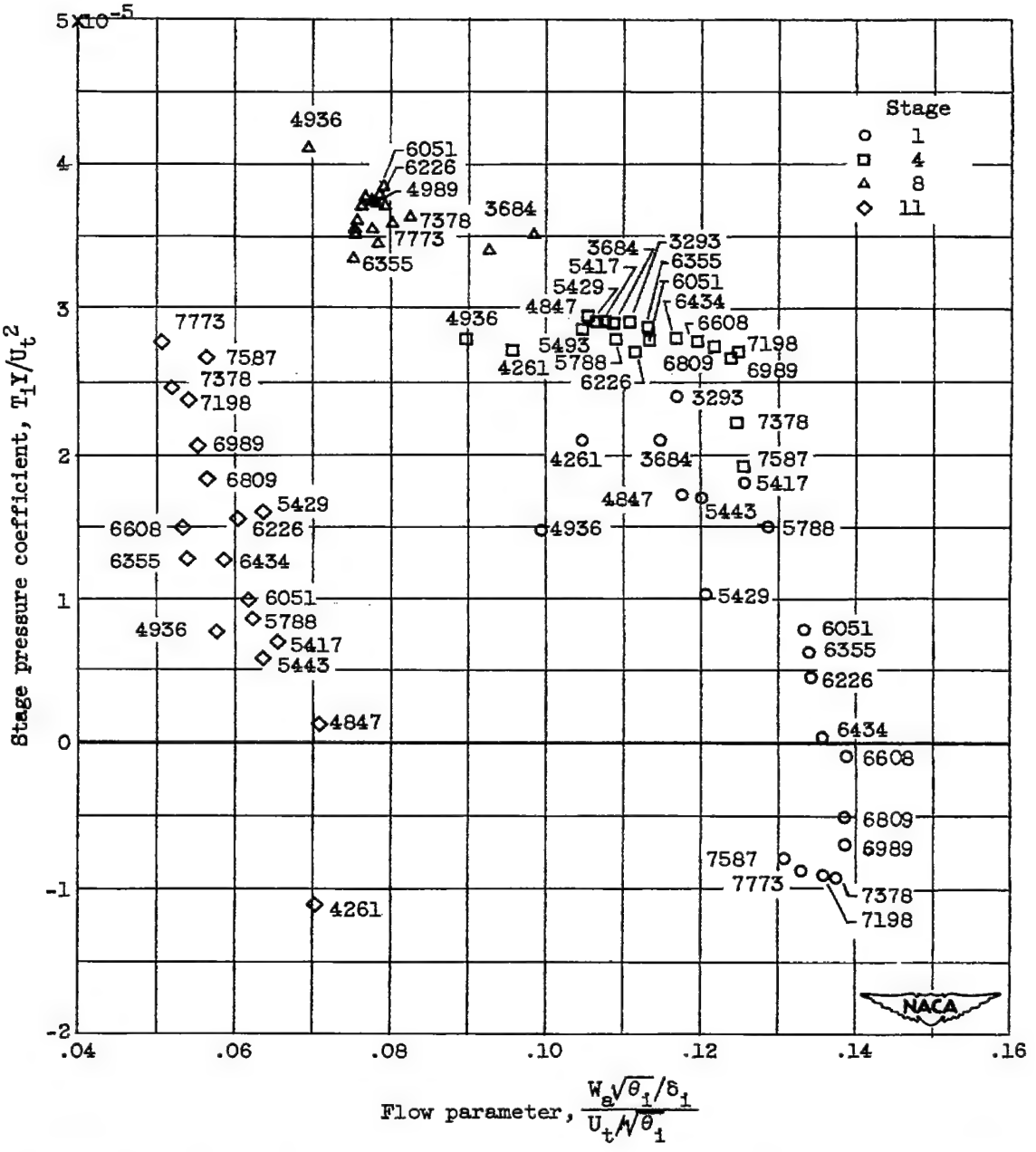

Figure 13. - Stage operating points for several stages of standard XJ40-WE-6 compressor for various equivalent engine speeds in rpm.

2616

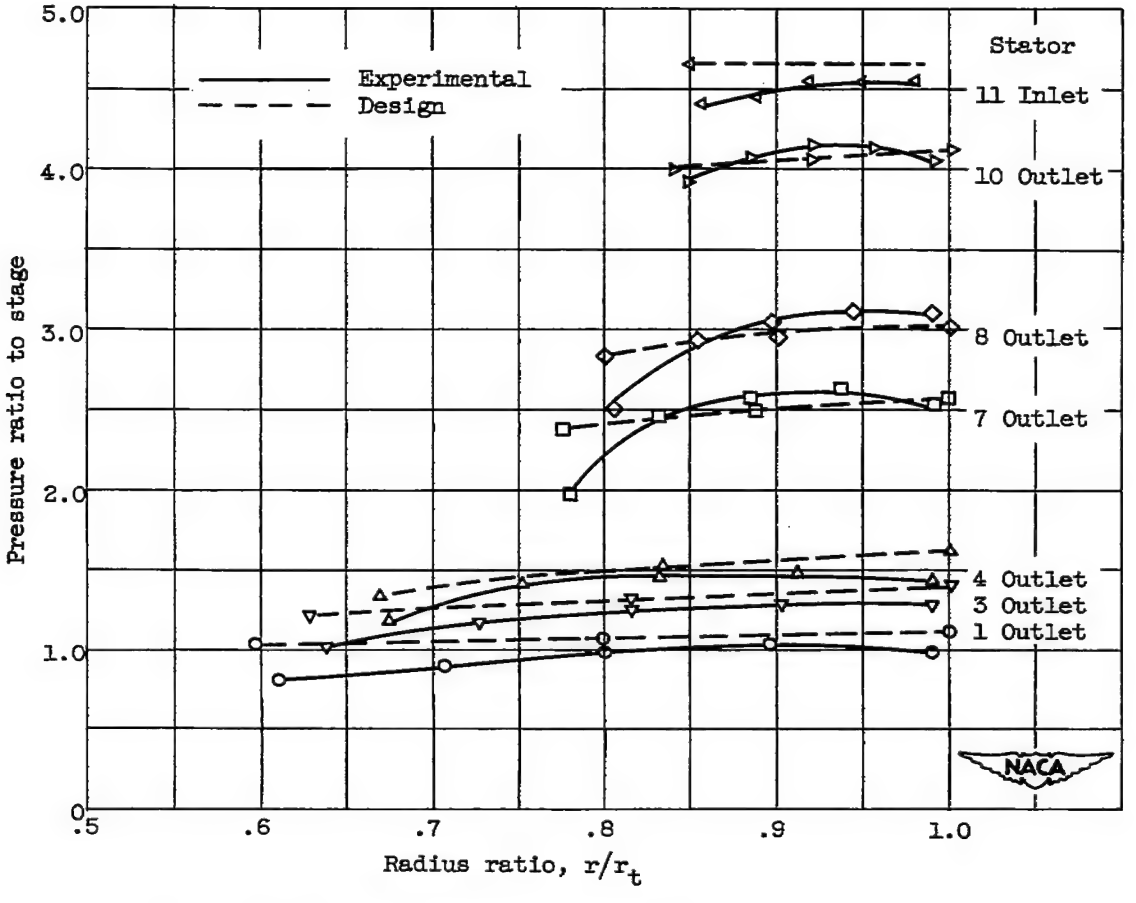

Figure 14. - Total-pressure-ratio distributions at several stator stations at an equivalent engine speed $N/\sqrt{\theta}$ of 7198 rpm.

[redacted]

2616

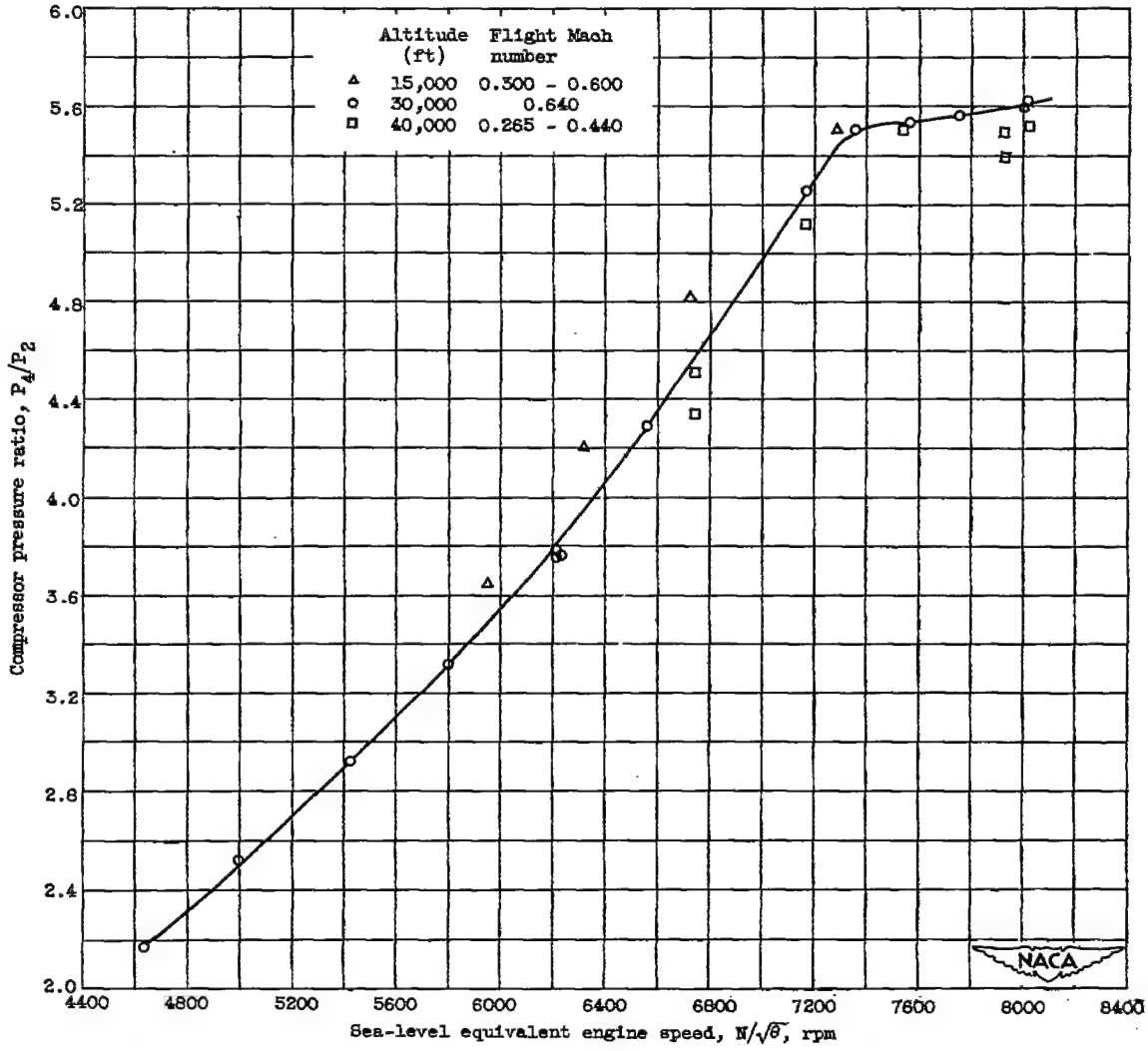

Figure 15. - Surge limit of standard compressor with mixer (configuration A).

2616

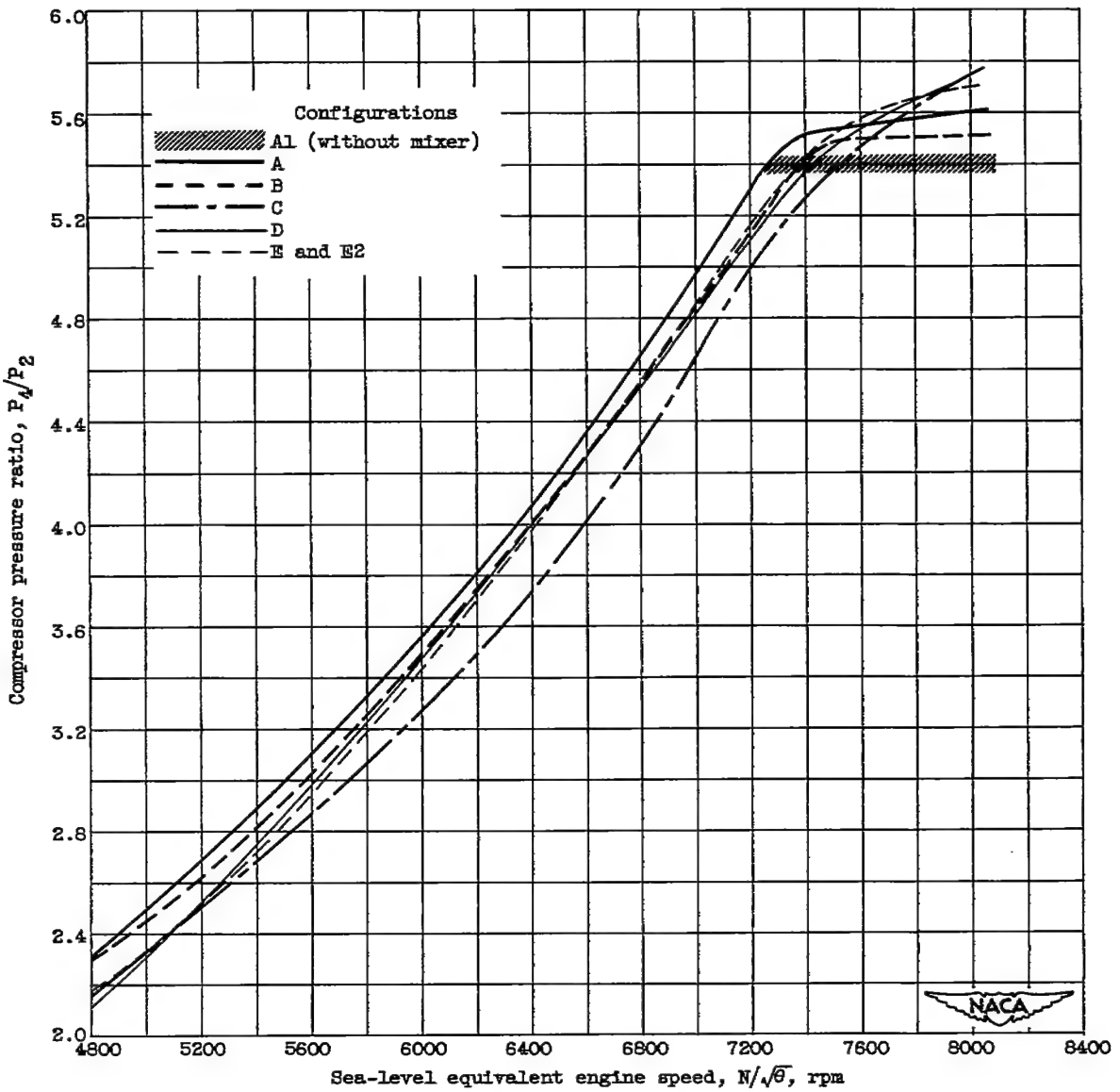

Figure 16. - Comparison of surge lines for the various compressor configurations investigated.

[redacted]

2616

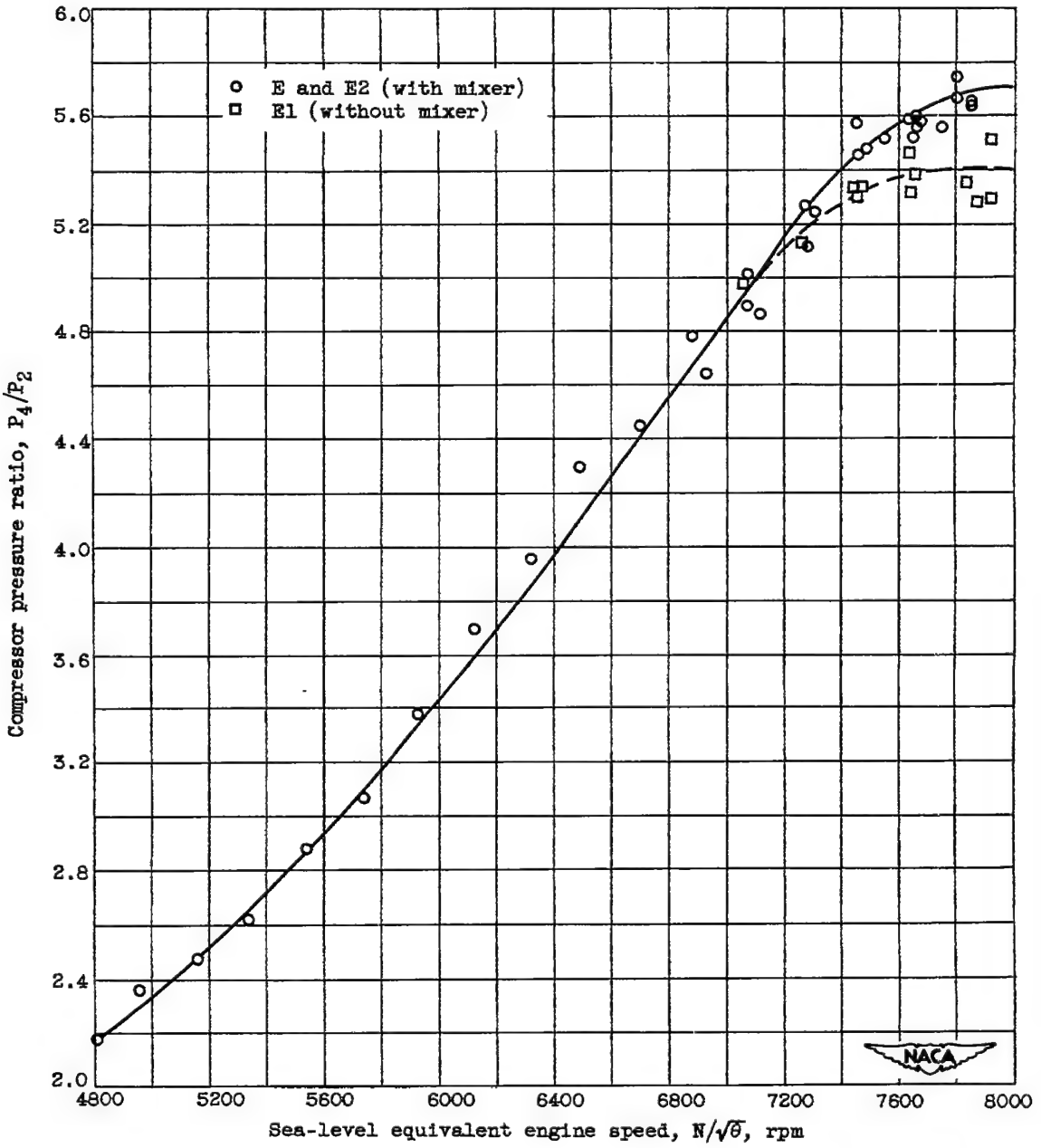

Figure 17. - Effect of mixer assembly at compressor outlet on surge limit of configuration E.

[redacted]

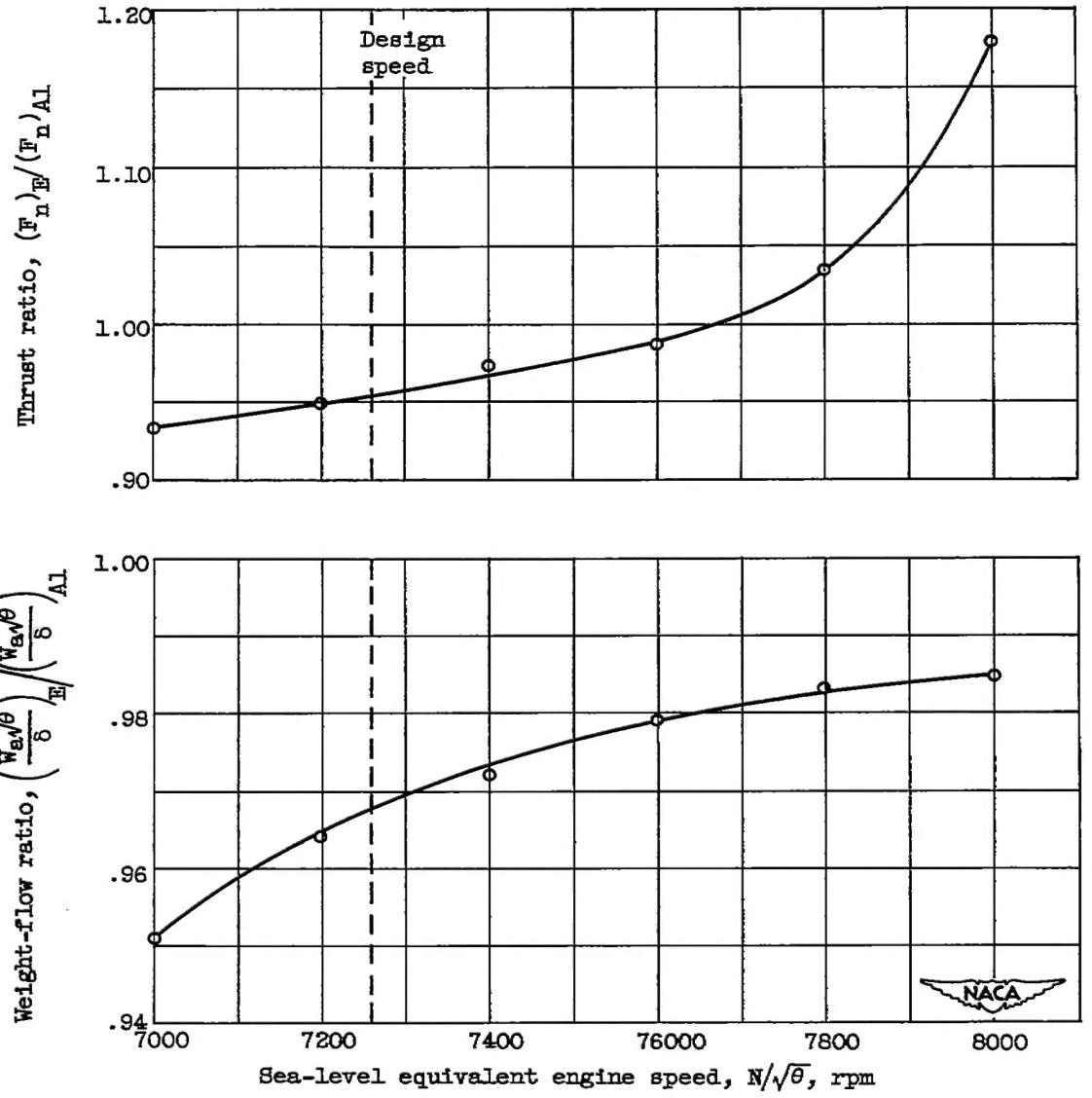

Figure 18. - Ratios of calculated net thrust and measured equivalent air flow for final and original compressor configurations. Altitude, 30,000 feet; flight Mach number, 0.64.

[redacted]

NASA Technical Library
3 1176 01435 6118

[redacted]